Direct Hydrothermal Synthesis of Highly Ordered Sn–SBA-15 Mesoporous Materials

Pallavi Shah,[1] Arumugamangalam V. Ramaswamy,[2] and Veda Ramaswamy*[1]
[1]*Catalysis Division, National Chemical Laboratory, Pune-411 008, India*
[2]*Department of Chemistry, University of Pune, Pune-411 007, India*

(Received April 13, 2006; CL-060441; E-mail: v.ramaswamy@ncl.res.in)

Well-ordered Sn^{4+}-incorporated mesoporous silica SBA-15 samples have been synthesized from tetraethyl orthosilicate (TEOS) and $SnCl_4$ (Si/Sn = 114–15) using nonionic surfactants under a slightly higher pH medium (optimum H_2O to HCl molar ratio) and characterized by XRD (an increase in lattice parameter), TEM (no SnO_2 species) and UV–vis spectral (absorption at 211 nm) techniques to show that Sn^{4+} ions are in tetrahedral coordination in Sn–SBA-15.

Incorporation of tin within the silica framework of many micro- and mesoporous molecular sieves is reported to impart in these materials interesting properties that make them useful as sensors, electrodes and catalysts.[1] There are many reports on the synthesis and characterization of mesoporous silicas with Sn and other semiconducting oxides in them, prepared either by direct synthesis or by post-synthesis procedures.[2] Among these mesoporous silicas, SBA-15 is thermally more stable than corresponding MCM-41.[3] Highly acidic conditions of preparation of Si–SBA-15 normally prohibit the incorporation of tin because of the high solubility of its precursors. During the preparation of metal-incorporated SBA-15 via post-synthetic methods, often metal oxides are formed in the channels or on the external surfaces. At least three different models of localized metal oxide particles within SBA-15 channels can be discerned.[4] Metal oxides formed in the mesopores may block the pores partially or fully, thereby reducing the surface area, pore volume, and pore diameter, or play a negative role in catalysis. It is still a challenge to find a one-step route of metal incorporation in SBA-15 in order to impart a catalytic functionality without changing its structural order or increasing the complexity of the synthesis. Recent reports suggest that structurally integral SBA-15, Al–, Co– and Fe–SBA-15 samples can be synthesized at slightly higher pH (2–5) conditions, provided the rate of hydrolysis of TEOS and condensation are controlled, for example, by adjusting the H_2O to HCl molar ratio of the synthesis gel.[5] Here, we report such a procedure in which the pH of the synthesis medium is varied by adjusting the H_2O/HCl ratio, while introducing Sn into SBA-15. The resulting materials may be useful in many applications, including as catalysts as reported earlier in transesterification reaction.[6]

An optimized procedure for the synthesis of Sn–SBA-15 molecular sieves has been worked out by changing the H_2O/HCl ratio and the resulting pH of the synthesis medium. Starting from a low H_2O/HCl ratio (pH < 1) and progressively increasing the ratio to 276, as reported by Vinu et al.,[5] then to 796 (70 mL of 0.07 M HCl) and without any addition of HCl in the synthesis media, we found that for a given Si/Sn (input) ratio of 100 to 10, a fixed water to HCl molar ratio of 796 (pH < 2) of the gel acidity leads to the formation of highly ordered Sn-containing mesoporous SBA-15 samples. For comparison,

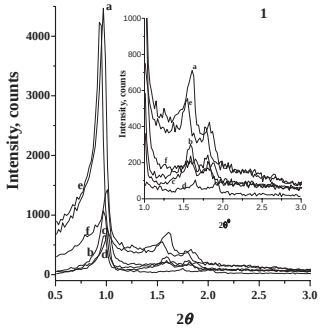

Figure 1. XRD patterns: (a) SBA-15, (b) Sn–SBA-15 (114), (c) Sn–SBA-15 (85), (d) Sn–SBA-15 (75), (e) Sn–SBA-15 (50), and (f) Sn–SBA-15 (15).

Sn-free SBA-15 was prepared by using a H_2O/HCl ratio of 796. The molar gel composition was 1TEOS:0.01–0.1SnO_2:0.016P123:0–0.46HCl:127H_2O. The solid products were recovered by filtration, dried and calcined at 823 K. The Sn–SBA-15 samples with different tin concentrations were characterized by XRD, N_2 adsorption, TEM, and UV–vis spectral techniques.

The powder XRD patterns of calcined Sn–SBA-15 samples with different Si/Sn ratios are similar to that of SBA-15 indicating a highly ordered mesoporous structure in all the samples as shown in Figure 1. It is interesting to note that the unit cell parameter increases significantly in Sn–SBA-15 samples with increasing tin content (Table 1). These values may indicate that the Sn^{4+} ions are incorporated into the framework of the SBA-15 materials, since the radius of the ionic Sn^{4+} is larger than that of Si^{4+} ($r_{Sn}{}^{4+} = 0.055$ nm and $r_{si}{}^{4+} = 0.026$ nm). XRD scan of samples in the high-angle region did not show the presence of crystalline SnO_2 or tin–silicate phases.

The UV–vis DR spectra of calcined Sn–SBA-15 samples were recorded to characterize the chemical nature and coordination spheres of the Sn species. The Sn–SBA-15 samples show a characteristic absorbance centered around 211 nm, which can be assigned to $O^{2-} \rightarrow Sn^{4+}$ transition, when Sn is in tetrahedral coordination in the framework. The intensity of this absorption increases with Sn content, as seen in Figure 2 and this provides a strong evidence for the incorporation of Sn^{4+} in SBA-15 structure. A weak absorption band at ≈248 nm may indicate the pres-

Table 1. Physicochemical characteristics of Sn–SBA-15 samples with different Si/Sn ratios

	Si/Sn		a	S_{BET}	S_{meso}	Vp	PD
	gel	EDX	/nm	/$m^2\,g^{-1}$	/$m^2\,g^{-1}$	/cm^3g^{-1}	/nm
SBA-15	—	—	10.2	906	445	1.04	4.6
Sn–SBA-15	100	114	10.5	920	516	1.22	5.3
Sn–SBA-15	80	85	10.4	948	560	1.32	5.6
Sn–SBA-15	60	75	10.9	976	609	1.39	5.7
Sn–SBA-15	40	50	10.9	1042	581	1.31	5.0
Sn–SBA-15	10	15	10.2	1127	777	1.62	5.7

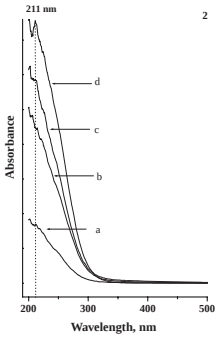

Figure 2. UV–vis spectra of (a) Sn–SBA-15 (114), (b) Sn–SBA-15 (85), (c) Sn–SBA-15 (75), and (d) Sn–SBA-15 (50).

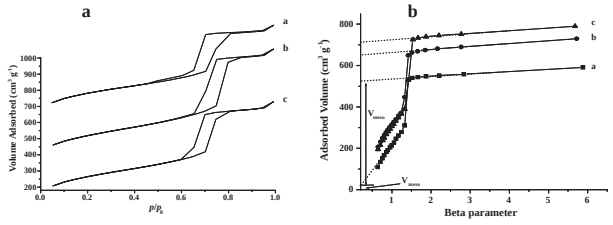

Figure 3. (**a**) N_2 adsorption/desorption isotherms and (**b**) β-plot of (a) SBA-15, (b) Sn–SBA-15 (75) and (c) Sn–SBA-15 (50).

ence of some Sn^{4+} ions in other coordination sphere. Sn–SBA-15 samples prepared using other (higher or lower) H_2O/HCl ratios show presence of Sn^{4+} essentially in octahedral coordination.[7]

The N_2 adsorption–desorption isotherms of Sn–SBA-15 samples are typically of irreversible type IV, with H1 hysteresis loop (Figure 3a). A significant and steady increase in the BET surface area with an increase in Sn content is observed for the samples (Table 1), which is due to an increase in the mesopore volume (from the β-plot[4]). The micropore volume is estimated to be about 19% in the parent SBA-15, which reduces to about 10% in Sn–SBA-15 having a Si/Sn ratio of 15 (Figure 3b). The mesopore diameter increases with increase in tin content. This is fairly a good indication of the presence of Sn in the corona region of the mesopore structure.

Under mild acidic conditions, the rate of condensation is faster than the rate of hydrolysis and, therefore, larger number of micropores is generated in Sn–SBA-15 samples. Sn–SBA-15 samples prepared under other pH conditions (lower H_2O to HCl ratios or in absence of any added HCl in the synthesis media) showed in general a decrease in the total surface area compared to parent SBA-15. In fact, there was a progressive decrease in the mesopore area with increasing Sn content, which may be due to occlusion of some SnO_2 in the mesopores of SBA-15.[7]

The TEM images (Figure 4) of Sn–SBA-15 samples show a well-ordered hexagonal array of mesopores with one-dimensional channels, which indicate a 2D hexagonal (*p6mm*) mesostructure. No individual tin oxide particles are observed at low Sn concentrations (Figures 4a–4c). For Sn–SBA-15 (15) sample, small, well-dispersed tin particles are observed (Figure 4d). Thus, by adjusting the H_2O/HCl molar ratio to 796, Sn gets incorporated into the lattice of SBA-15 at a low Sn concentrations (Si/Sn > 10), which is evidenced by XRD, TEM, and UV data.

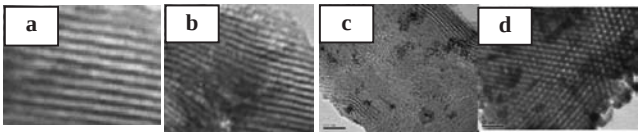

Figure 4. Transmission electron micrographs: (a) Sn–SBA-15 (85), (b) Sn–SBA-15 (75), (c) Sn–SBA-15 (50), and (d) Sn–SBA-15 (15).

At higher Sn concentrations, similar gel conditions lead to well-dispersed SnO_2 phase in SBA-15. By using a H_2O/HCl molar ratio of 276 as given in the literature,[5] SnO_2 agglomerates are formed in the channels or on the external surface, which block the pores partially, thereby reducing the surface area. In our earlier report,[6] we found that when SBA-15 was impregnated with Sn ions using $SnCl_4$ solution, there was a decrease in total surface area and pore volume due to some blockage of the mesopores. In comparison to the earlier procedures, the present method of preparation leads to an increase in total surface area (Table 1) that may indicate the presence of some Sn^{4+} ions as a part of the mesopores formed during the hydrothermal synthesis.

When P123 is mixed with water at room temperature, it forms micelles with PPO core and hydrated PEO coronas. The hydrophilic region of the surfactant is surrounded by halide ions forming an electrical double layer with a peripheral negative charge (S^+X^-). The formation of hexagonal mesophase under highly acidic conditions occurs through the $S^0H^+X^-I^+$ pathway. With increasing H_2O/HCl ratio, the charge on silica is reduced and the strength of interaction between the surfactant and the inorganic species I^+ will decrease. Hence, the system will be able to move to a more random structure. But this is compensated by the addition of $SnCl_4 \cdot 5H_2O$, which on hydrolysis at this pH produces HCl. TEOS and $SnCl_4 \cdot 5H_2O$ are hydrolysed and protonated in acidic medium forming ethanol, $\equiv Si–OH_2^+$, HCl, and $\equiv Sn–OH_2^+$. This positively charged silica species (I^+) are attracted electrostatically to the anionic portion of the surfactant ion pair (S^+X^-) forming electrical triple layer, where halide ions coordinate through Columbic interaction to the protonated silica groups. But with increasing the H_2O/HCl ratio, the concentration of tin hydroxy species increases. Hence, partially condensed silica species are able to form Sn–O–Si bond at this condition. The amount of Sn incorporation can, thus, be controlled by adjusting the molar H_2O/HCl ratio without affecting the structural ordering of SBA-15 materials.

References and Notes

1 a) N. K. Mal, A. V. Ramaswamy, *J. Mol. Catal. A: Chem.* **1996**, *105*, 149. b) A. Corma, L. T. Nemeth, M. Renz, S. Valencia, *Nature* **2001**, *412*, 423. c) G. Li, S. Kawi, *Sens. Actuators, B* **1999**, *59*, 1.
2 a) R. Ryoo, S. Jun, J. M. Rim, M. J. Kim, *Chem. Commun.* **1997**, 2225. b) A. Corma, M. T. Navarro, L. Nemeth, M. Renz, *Chem. Commun.* **2001**, 2190. c) Y. Teraoka, S. Ishida, A. Yamasaki, N. Tomonaga, A. Yasutake, J. Izumi, I. Moriguchi, S. Kagawa, *Microporous Mesoporous Mater.* **2001**, *48*, 151. d) K. Choudhary, T. K. Das, P. R. Rajmohanan, K. Lazar, S. Sivasankar, A. J. Chandwadkar, *J. Catal.* **1999**, *183*, 281.
3 D. Zhao, J. Feng, Q. Huo, N. Molish, G. H. Fredrickson, B. F. Chmelka, G. D. Stucky, *Science* **1998**, *279*, 548.
4 S. Perathoner, P. Lanzafame, R. Prassalacqua, G. Centi, R. Schlögl, D. S. Su, *Microporous Mesoporous Mater.* **2006**, *90*, 347.
5 a) A. Vinu, V. Murugesan, W. Böhlmann, M. Hartmann, *J. Phys. Chem. B* **2004**, *108*, 11496. b) A. Vinu, M. Hartmann, *Chem. Lett.* **2004**, *33*, 588. c) X. Cui, W. C. Zin, W. J. Cho, C. S. Ha, *Mater. Lett.* **2005**, *59*, 2257. d) Y. Li, Z. Feng, Y. Lian, K. Sun, L. Zhang, G. Jia, Q. Yang C. Li, *Microporous Mesoporous Mater.* **2005**, *84*, 41.
6 P. Shah, A. V. Ramaswamy, K. Lazar, V. Ramaswamy, *Appl. Catal., A* **2004**, *273*, 239; *Stud. Surf. Sci. Catal.* **2004**, *154*, 870.
7 P. Shah, V. Ramaswamy, unpublished results.

Published on the web (Advance View) July 1, 2006; doi:10.1246/cl.2006.860